FINITE ELEMENT ANALYSIS OF THE DEEP DRAWING PROCESS OF MAGNESIUM SHEETS

Dan Cătălin BÎRSAN

"Dunarea de Jos" University of Galati, Romania
email: dbirsan@ugal.ro

ABSTRACT

This study presents a finite element simulation of the deep drawing process applied to a 2-mm thick magnesium sheet using Simufact Forming. The forming operation was investigated under four different punch velocities, 10 mm/s, 20 mm/s, and 30 mm/s, to assess the influence of deformation speed on material response. The numerical results revealed distinct differences in stress distribution, effective plastic strain, and deformation pattern as a function of forming velocity. The simulations also produced force evolution curves along the Z direction, which demonstrated clear correlations between forming speed and required forming load. At lower speeds, material flow was more homogeneous with smoother strain gradients, whereas higher forming speeds resulted in intensified stress concentrations and more localized deformation. The analysis provides insight into the strain-rate-sensitive forming behavior of magnesium sheets and supports the selection of optimal forming conditions for improved manufacturability in lightweight structural applications.

KEYWORDS: magnesium sheet forming, FEM, deep drawing

1. INTRODUCTION

1.1. Review of clinching simulation methods

The deep drawing process is widely employed in the manufacturing of lightweight sheet-metal components, particularly in applications where weight reduction and mechanical performance are critical. Magnesium alloys, due to their exceptionally low density and favorable strength-to-weight ratio, are increasingly used in the automotive, aerospace, consumer electronics, and medical industries. Deep-drawn magnesium parts are found in structural housings, brackets, casings, protective covers, and energy-absorbing components. The process allows the production of complex geometries from flat sheet material while maintaining dimensional precision and material continuity. As industry trends continue to prioritize lightweight structures and fuel-efficient designs, the forming of magnesium sheets through deep drawing represents a key enabling technology for modern engineering applications.

However, forming magnesium sheets presents significant challenges due to their limited room-temperature ductility and pronounced strain-rate and temperature sensitivity. The deep drawing of magnesium often leads to localized thinning, cracking, or wrinkling if process parameters are not adequately controlled. In this context, finite element modelling (FEM) serves as a powerful tool for predicting stress–strain evolution, optimizing forming conditions, and mitigating failure risks. By simulating different forming speeds, material responses can be evaluated prior to manufacturing, enabling improved process design and enhanced formability for magnesium sheet components.

Research on the deep drawing of magnesium sheets has been extensively developed in the last two decades, supported both by experimental work and advanced finite element simulations. Magnesium alloys such as AZ31B are of particular interest due to their low density and their potential for lightweight engineering applications. However, their limited ductility at room temperature makes forming challenging, prompting numerous studies on process optimization.

Huang T-B. et co. [1] explored non-isothermal deep drawing of AZ31B magnesium sheet, using FEM to

demonstrate that elevating temperature improves formability. Their work established the strong temperature dependency of magnesium deformation and introduced simulation as a predictive tool before physical trials. Complementing this work, Yang [2] investigated elliptic cup deep drawing of magnesium alloy sheet through FEM analysis and showed how geometric asymmetry influences stress localization and thinning. This highlighted the importance of die geometry and sheet alignment on the integrity of the final part.

Further optimization strategies were introduced by Watiti and Labeas [3], who used FEM to fine-tune forming parameters such as punch speed and blank-holder force. Their results demonstrated that numerical optimization can significantly reduce failure risk and improve dimensional accuracy. Similarly, Palaniswamy and Ngaile [4] examined deep drawing of magnesium under elevated temperatures and provided evidence that thermo-mechanical modelling improves simulation fidelity in predicting flow stress and avoiding cracking.

Beyond process simulation, the formability and damage evolution of magnesium sheets have been studied in depth. Li et al. [5] analyzed the relationship between temperature and ductility of AZ31B sheets, demonstrating that higher temperatures increase elongation and delay fracture onset. Lee, Lee, and Wagoner [6] developed an improved constitutive model for magnesium sheet forming, capturing its unique hexagonal crystal structure behavior. Their work is widely applied in modern FEM simulations to ensure realistic stress–strain predictions.

Failure mechanisms were examined by Park and Kim [7], who analyzed thinning and fracture initiation during deep drawing of magnesium sheets and identified critical regions where rupture is most likely to occur. Their findings contribute to predictive defect-avoidance strategies in industrial forming.

At a deeper micro-mechanical modelling level, Kurukuri and Kuwabara [8] combined digital image correlation with FEM simulations to quantify anisotropy in magnesium sheet deformation. Their work established that rolling-induced texture leads to direction-dependent mechanical behavior, which must be incorporated into FEM models. Wagoner and Lee [9] further advanced the field by applying crystal plasticity models to magnesium sheet deformation, providing insight into the role of twinning and non-basal slip at various strain rates. Complementarily, Jain and Sachdev [10] investigated forming behavior and constitutive modelling of magnesium alloys, offering valuable parameters for FEM models used in predicting failure and optimizing tool design.

Overall, current research demonstrates that magnesium sheet forming is highly sensitive to processing parameters, including strain rate, forming speed, temperature, and anisotropy. While the influence of temperature has been extensively studied,

the specific role of forming velocity on stress evolution, plastic strain distribution, and forming loads has received comparatively less attention. This motivates the present numerical investigation, which systematically varies punch speed and evaluates its effect on the deep drawing of magnesium sheets using finite element modelling.

2. METHODOLOGY AND MATERIAL MODEL DEFINITION

2.1. Simulation framework and model setup

The deep drawing simulations were carried out using the commercial finite element software Simufact Forming, which provides an explicit dynamic solution scheme suitable for large plastic deformation problems. The model consisted of a deformable magnesium blank with a thickness of 2 mm, together with rigid analytical tooling elements, including punch, die, and blank-holder. Treating the tools as rigid bodies reduced computational cost while preserving realistic contact behaviour.

Boundary conditions were defined to replicate the actual forming sequence. The lower die was fully constrained, while the blank-holder applied a constant normal pressure to prevent wrinkling and ensure proper material confinement. The punch displacement was prescribed as a kinematic input along the Z-axis, with four discrete forming velocities investigated: 10 mm/s, 20 mm/s, and 30 mm/s. These speeds were selected to examine the influence of deformation rate on strain localization, stress development, and required forming force.

Surface interactions between sheet and tools were modelled using a Coulomb friction formulation with a calibrated friction coefficient typical for magnesium sheet forming. A refined mesh was applied in the critical deformation zone of the blank—particularly near the punch radius and die edge—where large strain gradients were expected. Mesh convergence checks ensured that further refinement would not significantly affect predicted strain and stress outcomes.

This modelling setup enabled the tracking of stress distribution (von Mises), effective plastic strain, and punch force evolution throughout the forming process, providing a reliable computational basis for analysing the strain-rate sensitivity of the magnesium sheet.

2.2. Material model definition

The magnesium sheet was modelled using an elastoplastic constitutive formulation suitable for large strain deformation. The elastic region was defined by linear isotropy, employing a Young's modulus of approximately 45 GPa and Poisson's ratio of 0.35, consistent with reported values for AZ-series

magnesium alloys. Beyond the elastic limit, yielding was governed by a von Mises criterion with isotropic strain hardening, allowing the model to capture the progressive reduction in flow stress slope as plastic deformation accumulated.

Because magnesium alloys exhibit pronounced sensitivity to deformation rate, particularly through activation of non-basal slip systems and twinning, strain-rate effects were incorporated into the flow rule. Plastic deformation was captured using a von Mises yield criterion combined with isotropic hardening. The mathematical model describing the material's behavior is as follows:

$$\sigma_F = C \cdot \dot{\varepsilon}^M \qquad (1)$$

Figure 1 illustrates the dependence of flow stress on strain rate for magnesium sheet material, showing that higher strain rates significantly increase flow stress, while elevated temperatures reduce resistance to deformation. The curves further demonstrate the combined influence of temperature, strain rate, and accumulated strain on the material's plastic response.
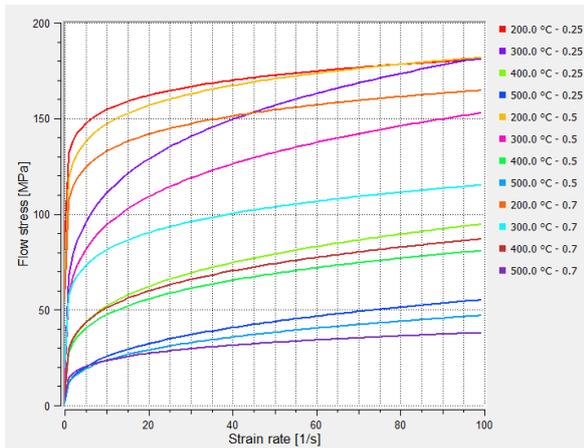
Fig. 1. *Flow stress as a function of strain rate at different temperatures and strain levels for magnesium alloy*

Thermal coupling was neglected due to the relatively short duration of the forming process and the absence of external heating sources, which result in minimal internal heat generation from plastic work. However, the selected constitutive model remains compatible with future thermo-mechanical extensions, should warm forming conditions be considered in subsequent studies.

The sheet was modeled as a deformable body, while the tool and support components, considering the materials used (tool steel and carbon steel), were treated as rigid bodies. Two-dimensional elements, specifically designed for axisymmetric analysis, referred to as Quad (10) in Simufact Forming terminology, were used to construct the model.

The tool velocity displacements were set to vary between 10, 20, and 30 mm/s, and the stroke was set to 20 mm. An automatic remeshing function was employed to regenerate the mesh and allow the simulation to continue with the updated configuration.

A structured mesh refinement strategy was applied to ensure sufficient resolution in regions of high deformation. The mesh was locally refined around the punch radius, die edge, and flange transition zone, where steep strain gradients and necking tendencies were expected to occur during deep drawing. In contrast, areas of the blank located far from the main deformation zone were meshed more coarsely to reduce computational cost. The mesh density was selected so that the smallest element size in the critical region was sufficiently small to capture strain localization and stress concentration without excessive numerical noise.
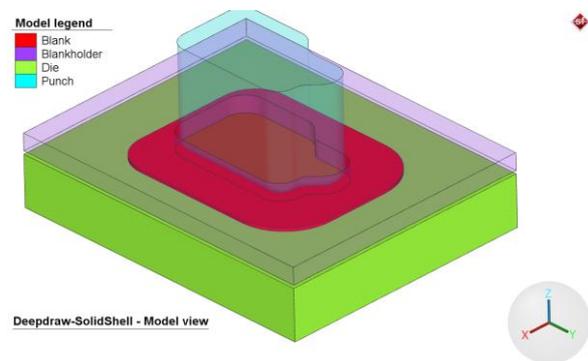
Fig. 2. *3D finite element model*

To evaluate mesh dependency, a sensitivity analysis was performed by conducting simulations with progressively refined meshes. The monitored outputs included peak punch force, maximum von Mises stress, and local effective plastic strain in the interlock region. The results showed that beyond a certain mesh resolution threshold, further refinement produced minimal variation in these key parameters (less than approximately 2–3% deviation). This indicates that the chosen mesh configuration provides convergence in both force response and stress–strain prediction.

3. RESULTS AND DISCUSSION

3.1. Stress and strain analysis

The stress distributions obtained from the simulations show a clear dependence on forming speed. At lower punch velocities, 10 mm/s, the von Mises stress is distributed more evenly across the deformation zone, with moderate concentration around the punch radius and die edge. In contrast, at higher forming speeds (20–30 mm/s), stress localization becomes more pronounced in the same regions, with peak values increasing due to strain-rate-induced material hardening. These concentrated zones indicate regions where micro-damage and thinning are most likely to initiate.

At 10 mm/s, Figure 3, the stress distribution shows a relatively smooth and broad spread of stresses across the formed cup. Moderate stress values dominate the surface with only limited regions of higher stress concentration, indicating that the material has sufficient time to redistribute during forming. The walls deform more uniformly, showing lower risk for localized thinning and fracture.

At 20 mm/s, Figure 4, the stress pattern begins to intensify with sharper gradients. Several isolated stress hotspots appear around the wall curvature and corner transitions, reflecting more localized deformation resistance. This marks the transition from ductile redistribution toward strain-rate-driven material stiffening.

At 30 mm/s, Figure 5, the stress field becomes increasingly concentrated, with higher peak stress bands visible along the cup walls and near the bottom fillet region. The stress localization is more pronounced, reflecting reduced material flow capability and increased internal hardening under rapid deformation.

This progressive stress intensification with forming speed confirms that magnesium, being strain-rate sensitive, hardens rapidly when deformation occurs too quickly. Consequently, high punch speeds cause the material to resist flow, resulting in intensified stress pockets that correspond directly to potential structural weaknesses.
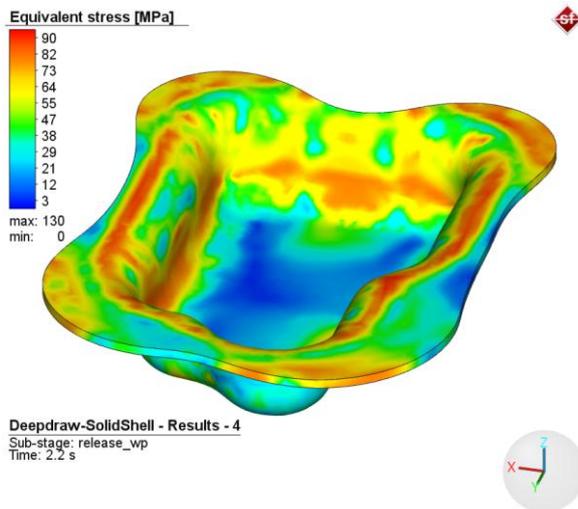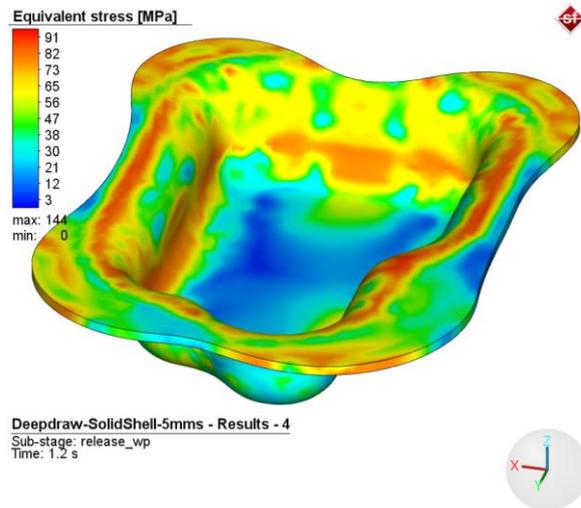

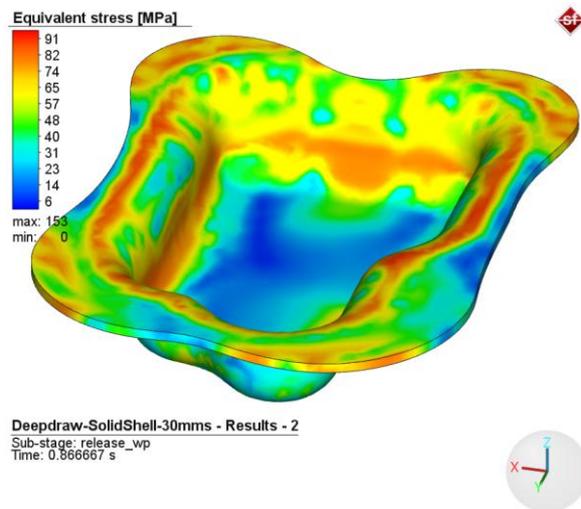**Fig. 4.** *VM stress at lower forming speed, 20mm/s*



Fig. 5. *VM stress at lower forming speed, 30mm/s*

3.2. Plastic strain analysis

At the lower forming speed, the plastic strain field appears broader and more diffusely distributed. The strain is spread over a larger volume of material, particularly around the punch indentation region and along the sheet interface. The maximum recorded effective plastic strain reaches approximately 2.60, but the high–strain area (red zone) is thicker and more evenly distributed across the interlocking region. This suggests that the material had more time to flow and conform to the cavity under slow deformation, resulting in a more homogeneous strain distribution but slightly lower material compaction in the joint.


Fig. 3. *VM stress at lower forming speed, 10mm/s*
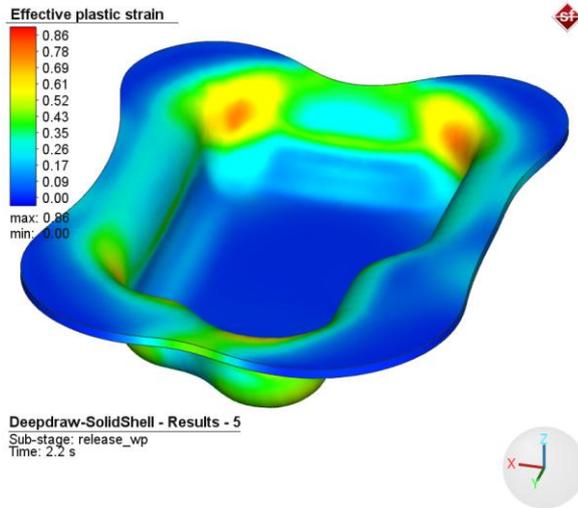
Fig. 6. *Plastic strain at 10 mm/s speed*

When comparing the effective plastic strain across the three forming speeds, a clear trend emerges: at 10 mm/s, the deformation spreads broadly over the entire surface of the sheet, producing diffuse and smooth strain gradients that indicate controlled material flow and accommodating deformation mechanisms. At 20 mm/s, the strain begins to concentrate into narrower regions, signaling the onset of strain localization and a reduced capacity of the material to redistribute deformation uniformly. This effect becomes even more pronounced at 30 mm/s, where plastic strain accumulates sharply in highly localized zones, particularly along the walls and die radius, demonstrating that the magnesium sheet stiffens under rapid loading and is unable to adjust plastically at high strain rates. Therefore, the increase in forming speed leads to a progressive reduction in strain uniformity, moving from distributed deformation at low speeds to concentrated strain bands at high speeds, with corresponding implications for thinning risk and failure susceptibility.
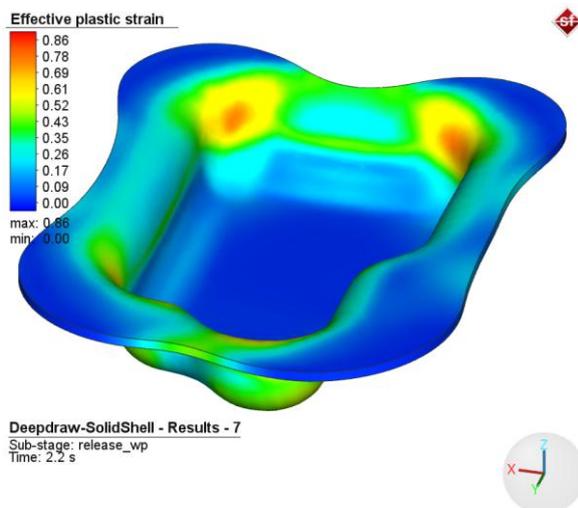

Fig. 7. *Plastic strain at 10 mm/s speed*

The graph, Figure 8, shows a continuous increase in effective plastic strain over time during the forming process, indicating steady and progressive plastic deformation of the magnesium sheet. At the early stage of forming, the strain gradually increases, reflecting initial resistance to deformation. As time progresses, the slope of the curve becomes slightly steeper, demonstrating accelerated deformation as the material undergoes larger strain accumulation. The smooth and monotonic nature of the curve suggests the absence of abrupt strain jumps or instability phenomena, implying that deformation occurred in a controlled manner without sudden localized fracture or abrupt yielding.
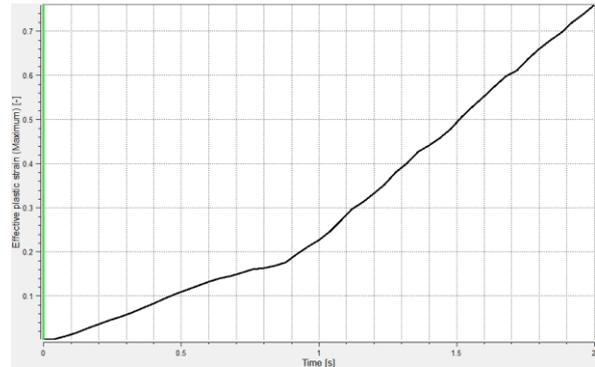
Fig. 8. *Effective plastic strain over forming time*

The graph, Figure 9, illustrates the evolution of vertical force in the punch and blankholder throughout the forming process. The force exerted by the punch (red curve) increases gradually over time, reflecting the progressive engagement of the material as it conforms to the die geometry. This smooth increase corresponds to steadily growing plastic resistance of the sheet as deformation deepens. The curve reaches a maximum around approximately 1.4–1.5 seconds, after which a slight drop is observed, indicating a reduction in forming resistance once the material has largely adopted its final shape and further displacement yields smaller incremental strain.

In contrast, the blankholder force (purple curve) exhibits a very rapid rise at the beginning of the process, reaching its peak value almost immediately. This behaviour reflects the initial clamping action required to restrain sheet movement and prevent wrinkling at the flange. After reaching this maximum, the blankholder force gradually decreases, which suggests that as the deformation progresses and material flow becomes more stable, less holding pressure is needed to maintain sheet stability and prevent buckling. The gradual decline of the blankholder force is consistent with the reduced lateral sheet flow as the blank transitions from flat sheet to formed geometry.
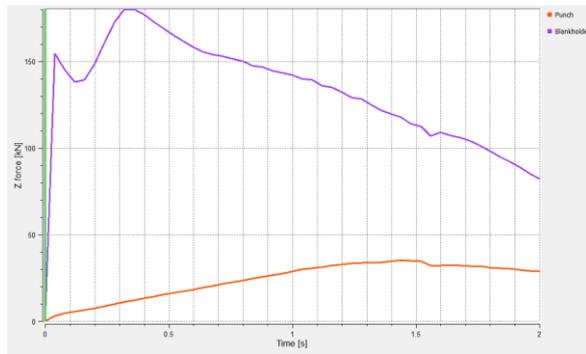
Fig. 9. *Force–time response during numerical pull-out tests for joints formed at 10 mm/s*

The contrasting behaviour of the two curves reflects their distinct mechanical roles: the punch provides forming energy and sees increasing resistance until shaping is complete, while the blankholder initially provides restraining force but reduces its contribution as material confinement becomes self-stabilized by geometry.

4. CONCLUSIONS

This numerical study assessed the influence of punch speed on the deep drawing process of a 2 mm magnesium sheet using finite element simulations in Simufact Forming. Three forming velocities were investigated: 10 mm/s, 20 mm/s, and 30 mm/s. The results demonstrated a consistent increase in stress concentration and strain localization with increasing forming speed. At the lowest speed of 10 mm/s, stress and effective plastic strain were more uniformly distributed across the cup geometry, indicating favourable material flow, reduced resistance, and a lower likelihood of local thinning or tearing.

As the forming speed increased to 20 mm/s, the deformation behaviour transitioned toward localized strain accumulation, with stress gradients intensifying in critical geometric regions. At the highest speed of 30 mm/s, these effects were amplified, producing sharply defined strain bands and higher peak stress values. This confirms that magnesium exhibits pronounced strain-rate sensitivity, becoming stiffer and less compliant under rapid loading, which restricts deformation homogeneity and introduces potential risks of material failure.

The force–time responses further supported these observations: the punch force gradually increased with forming depth and reached a maximum before slightly declining as deformation stabilized, while the blankholder force peaked early during the initial clamping phase and subsequently decreased as material flow became constrained by geometry rather than external holding pressure.

The findings reveal that forming speed is a key process parameter controlling the stress–strain evolution in magnesium sheet forming. Moderate forming velocities, close to 10 mm/s, are more favourable for stable and uniform deformation, whereas excessive speeds, such as 30 mm/s, lead to hardening, intensified stress concentration, and reduced formability. These insights highlight the need for optimized forming rates in industrial applications to ensure high-quality deep-drawn magnesium components.

REFERENCES

[1]. Huang T-B., Tsai Y-A., Chen F-K., *Finite element analysis and formability of non-isothermal deep drawing of AZ31B sheets*, Journal of Materials Processing Technology, Vol. 177, 142–145, 2006.

[2]. Yang T.S., *Finite element analysis of elliptic cup deep drawing of magnesium alloy sheet*, Journal of Achievements in Materials and Manufacturing Engineering, Vol. 27, Issue 2, 143–146, 2008.

[3]. Watiti V.B., Labeas G.N., *Finite element optimization of deep drawing process forming parameters for magnesium alloys*, International Journal of Material Forming, Vol. 3, 97–100, 2010.

[4]. Palaniswamy H., Ngaile G., *Finite element simulation of magnesium alloy sheet forming at elevated temperatures,* Journal of Manufacturing Processes, Vol. 6, Issue 1, 14–26, 2004.

[5]. Li Z., Dong Y., Lin Z., *Formability of AZ31B magnesium alloy sheet at elevated temperatures*, Materials Science and Engineering A, Vol. 523, 75–82, 2009.

[6]. Lee J.Y., Lee M.G., Wagoner R.H., *A practical constitutive equation for magnesium alloy sheet forming*, International Journal of Plasticity, Vol. 46, 54–67, 2013.

[7]. Park T.H., Kim D.H., *An investigation on failure prediction in deep drawing of AZ31B magnesium alloy*, Metals and Materials International, Vol. 19, 1185–1192, 2013.

[8]. Kurukuri S., Kuwabara T., *Digital image correlation and FEM study of anisotropy in AZ31 magnesium alloy sheet forming*, International Journal of Solids and Structures, Vol. 47, 1672–1680, 2010.

[9]. Wagoner R.H., Lee M.G., *Crystal plasticity modelling of magnesium sheet deformation*, Scripta Materialia, Vol. 68, 587–590, 2013.

[10]. Jain M., Sachdev A.K., *Forming behavior and constitutive modelling of magnesium alloys for sheet forming applications,* Journal of Materials Engineering and Performance, Vol. 17, 101–108, 2008.